Analysis of Three-Phase Induction Motors Controlled by Thyristors

Analysis of Three-Phase Induction Motors Controlled by Thyristors

Tomoo FUJII*, Masao WATANABE** and Takemitsu ISHIZAKI*

(Received June 15, 1971)

This paper deals with an analytic means of the three-phase induction motor whose primary voltage is controlled by symmetrical triggering of inverse parallel connected pairs of thyristors series with stator windings. On this control, the motor exciting voltage waveforms become segments of sinusoids and the phase currents are discrete ones. Operational modes of this motor control may be divided into two modes; three-phase operation and single-phase operation.

Motor characteristics are obtained through the Fourier analysis of the voltage waves on each modes. And the influences of the harmonic components of the supply voltage on the motor characteristics are investigated.

1. Introduction

As the thyristors of high current and voltage ratings become available at decreasing cost, it is finding increased use in the control of polyphase induction motors. There are two main areas of application. One of these is the use of thyristor inverter circuits to form an effective variable-frequency supply to the motor[1),2)], and the other is the use of inverse parallel connected pairs of thyristors series with the stator winding, (hereafter referred to as the thyristor pair), to form an effective variable-voltage supply to the motor.[3)~10)],

This paper presents the primary voltage control using thyristor pair, which is one of the latter application that is useful for low power induction motor controls. The waveforms of the motor exciting voltage controlled by symmetrical triggering of thyristor pair are segments of sinusoids. Therefore the motor exciting voltage is rich in higher harmonics.

The influence of these harmonics can easily be investigated by knowing the rate of each harmonic, which is obtained from an expansion of voltage waveforms in a Fourier series.

Two of the representative operational modes occur within this control as follows,

mode I : normal three-phase operation, and in this mode the motor speed can be controlled smoothly by adjusting exciting voltage,

mode II : single-phase operation, and in this mode the motor per se has no starting torque.

The boundary of these modes is the function of triggering angle, current conducting

* Department of Electrical Engineering, College of Engineering.
** Graduate Student, Department of Electrical Engineering, College of Engineering.

angle, and the power factor angle of the motor equivalent circuit per phase.

2. Abstract of the Primary Voltage Control

Control of the primary voltage of the induction motor has been made through the technology concerning semiconductors. The fundamental principle of the primary voltage control is that the generated torque which corresponds to the speed is proportional to square of the supply voltage with voltage variation.

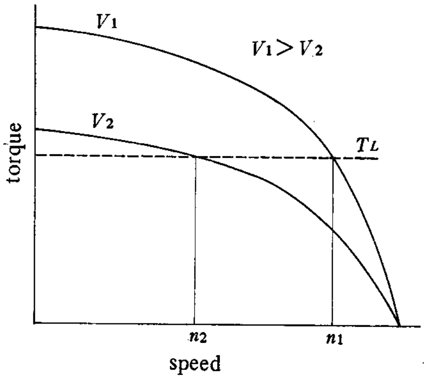

Fig. 1. Schematic speed vs. torque characteristics of three-phase induction motor with voltage variation. Dotted line shows load torque.

As shown in Fig. 1, the generated torque exists in equilibrium with load torque T_L at the speed n_1 in the voltage V_2. But when the voltage is reduced to V_2, its equilibrium state is reached at reduced speed n_2. This is the basic principle of the variable speed operation of induction motors controlled by the primary voltage control.

In this reserch, thyristor pair is used to give the primary voltage control.

3. Analysis

A connection of main circuit to give symmetrical control of a star connected three-phase induction motor is shown in Fig. 2.

The foregoing analysis are based on the equivalent circuit of the motor. Equivalent circuit for a three-phase induction motor may be reduced to resistance-inductance series circuit. When a sinusoidal voltage controlled by thyristor pair is impressed on this circuit, the relation among triggering angle α, current conducting angle β and power factor angle φ is given in eq. (1).

$$\sin(\alpha+\beta-\varphi) = \sin(\alpha-\varphi)\,\varepsilon^{-R/(\omega L)\beta} \qquad (1)$$

where

$$\varphi = \tan^{-1}\frac{\omega L}{R}, \quad R, L\text{: equivalent circuit resistance and inductance,}$$

$\omega = 2\pi f$, f: line frequency.

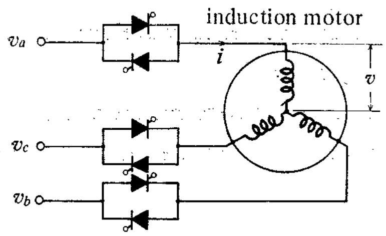

Fig. 2. Main circuit of "thyristor-pair" —induction motor drive.

Phase control can be done for $\varphi \leq \alpha \leq \pi$, in this region the line current is discontinuous. Relations of α vs. β with various power factor angle φ are shown in Fig. 3.[9] They are obtained by numerical solutions of eq. (1).

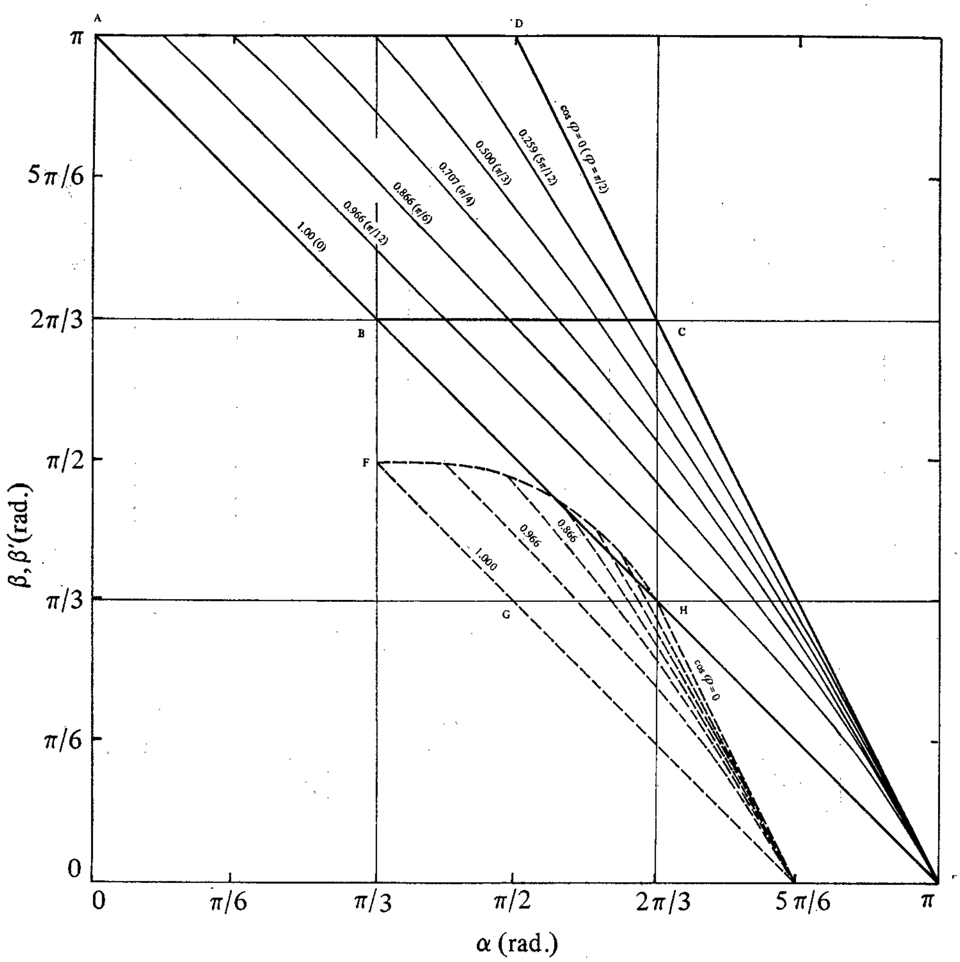

Fig. 3. Relations of α vs. $\beta(\beta')$with various φ.

3-1. Operational Mode and Exciting Voltage Waveform.[9),10)]

Typical line-to-neutral stator winding voltage waveforms on Fig. 2 are shown in Figs. 4~7. Fig. 4 and Fig. 5 are theoretical waveforms and Fig. 6 and Fig. 7 are oscillograms corresponds to Fig. 4 and Fig. 5.

In Fig. 6 and Fig. 7, line current waveforms are also shown.

As shown in Fig. 4, voltage waveforms are series of segments of sinusoidal line-to-neutral voltage V, line-to-line voltage $\frac{\sqrt{3}}{2}V\varepsilon^{j(\pi/6)}$ and $\frac{\sqrt{3}}{2}V\varepsilon^{-j(\pi/6)}$.

These voltage waveforms will maintain for $\frac{2}{3}\pi<\beta<\pi$ and $\varphi<\alpha\leq\frac{2}{3}\pi$, as shown by the area ABCD in Fig. 3.

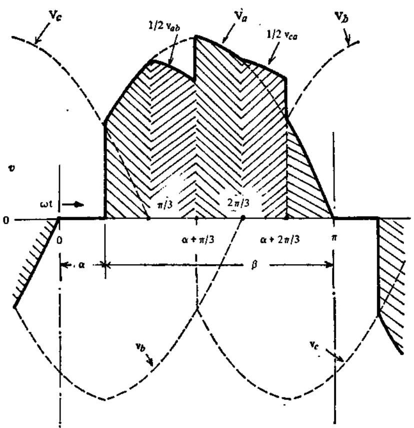

(a) $\alpha=\pi/6$, $\varphi=0$

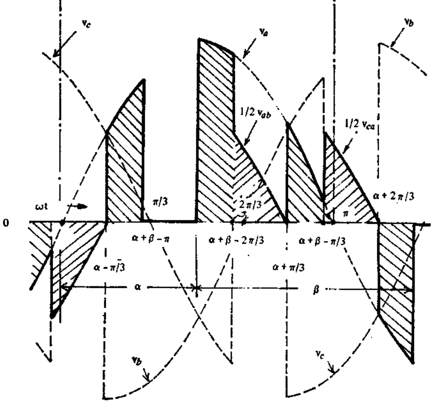

(b) $\alpha=\pi/2$, $\varphi=\pi/3$

Fig. 4. Theoritical waveforms of stator exciting voltage in mode I.
(a): resistive load,
(b): inductive load.

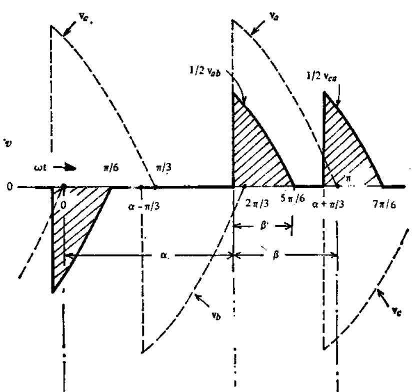

(a) $\alpha=11\pi/18$, $\varphi=0$

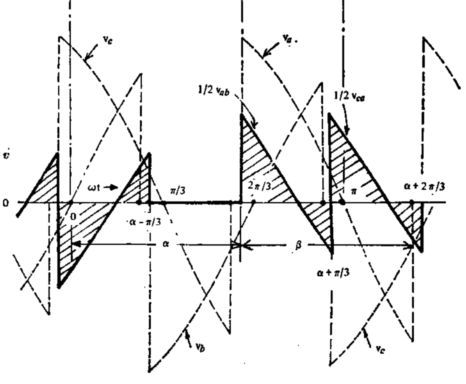

(b) $\alpha=11\pi/18$, $\varphi=\pi/3$

Fig. 5. Theoritical waveforms of stator exciting voltage in mode II.
(a): resistive load,
(b): inductive load.

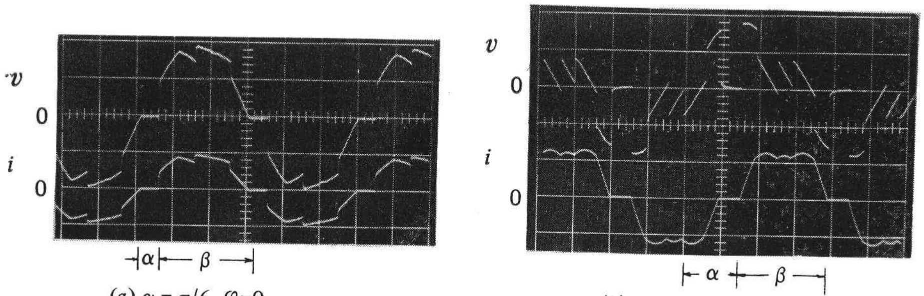

(*a*) $\alpha=\pi/6$, $\varphi=0$　　(*b*) $\alpha=\pi/2$, $\varphi=\pi/3$

Fig. 6. Oscillograms of voltage and current waveforms corresponding to Fig. 4. (a): resistive load, (b): inductive load.

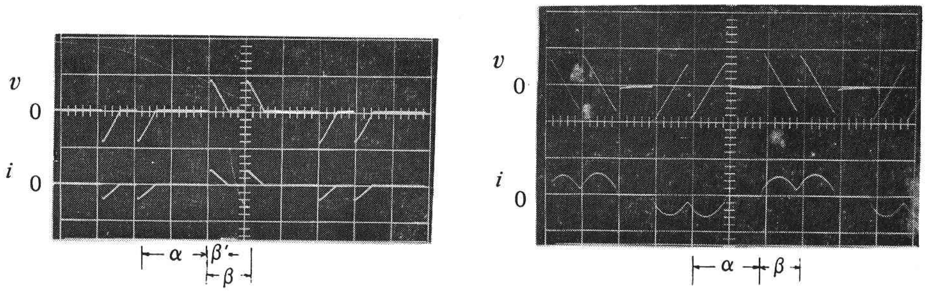

(a) $\alpha=11\pi/18$, $\varphi=0$　　(b) $\alpha=11\pi/18$, $\varphi=\pi/3$

Fig. 7. Oscillograms of voltage and current waveforms corresponding to Fig. 5. (a): resistive load, (b): inductive load.

In this region, motor stator winding has a period impressed by the three-phase line voltage simultaneously. Therefore the motor can operate as an ordinary three-phase induction motor.

In Fig. 5, voltage waveforms are series of segments of sinusoidal line-to-line voltage $\frac{\sqrt{3}}{2}V\varepsilon^{j(\pi/6)}$ and $\frac{\sqrt{3}}{2}V^{-j(\pi/6)}$, and line-to-neutral voltage V disappears. This means that the motor stator winding is excited only by line-to-line voltage at any instant, and the motor operates on the condition of the single-phase operation and per se has no starting torque. This single-phase operation occurs for $0\leq\beta\leq\frac{2}{3}\pi$, $\frac{\pi}{3}\leq\alpha\leq\pi$ as shown by the area BEC in Fig. 3.

Because of the line-to-line voltage leads the line voltage by the time-phase angle $\frac{\pi}{6}$, the triggering angle referred to the line-to-line voltage becomes $\alpha+\frac{\pi}{6}$.

Therefore the stator winding voltage will be zero at $\alpha=\frac{5}{6}\pi$ and also conduction angle must be read corresponding to this leading triggering angle. These relations are shown in dotted line in Fig. 3. Here we define the former operational mode to mode I, and the latter one to mode II.

3-2. Analysis of Exciting Voltage Waveforms

In order to investigate the performance of an induction motor whose exciting voltage is nonsinusoidal waveform, it is one of available methods to know the rate of harmonics by Fourier analysis. The Fourier series for exciting voltage waveform in mode I, Fig. 4, is as follows,

$$v_I(t) = \frac{3}{\pi}\sqrt{2}\,V\left\{\sqrt{A_I^2+B_I^2}\sin(\omega t+\gamma_I)+\sum\frac{1}{k^2-1}\sqrt{C_I^2+D_I^2}\sin(k\omega t+\delta_I)\right\} \tag{2}$$

where

$$A_I = \frac{1}{4}\left\{\left(2\beta-\frac{2}{3}\pi\right)\cos\alpha+\sin\alpha-\sin(2\beta+\alpha)\right\}$$

$$B_I = \frac{1}{4}\left\{\left(2\beta-\frac{2}{3}\pi\right)\sin\alpha+\cos\alpha-\cos(2\beta+\alpha)\right\}$$

$$\begin{aligned} C_I = \frac{1}{3}\Big[&\sin(\alpha+\beta)\left\{-k\cos\left(k\beta-\frac{2}{3}k\pi\right)+k\cos\left(k\beta-\frac{k}{3}\pi\right)+2k\cos k\beta\right\} \\ &+\cos(\alpha+\beta)\left\{\sin\left(k\beta-\frac{2}{3}k\pi\right)-\sin\left(k\beta-\frac{k}{3}\pi\right)-2\sin k\beta\right\} \\ &+\sin\alpha\left(-2k-k\cos\frac{k}{3}\pi+k\cos\frac{2}{3}k\pi\right) \\ &+\cos\alpha\left(\sin\frac{k}{3}\pi-\sin\frac{2}{3}k\pi\right)\Big] \end{aligned}$$

$$\begin{aligned} D_I = \frac{1}{3}\Big[&\sin(\alpha+\beta)\left\{k\sin\left(k\beta-\frac{2}{3}k\pi\right)-k\sin\left(k\beta-\frac{k}{3}\pi\right)-2k\sin k\beta\right\} \\ &+\cos(\alpha+\beta)\left\{\sin\left(k\beta-\frac{2}{3}k\pi\right)-\sin\left(k\beta-\frac{k}{3}\pi\right)-2\sin k\beta\right\} \\ &+\sin\alpha\left(k\sin\frac{k}{3}\pi-k\sin\frac{2}{3}k\pi\right) \\ &+\cos\alpha\left(2+\cos\frac{k}{3}\pi-\cos\frac{2}{3}k\pi\right)\Big] \end{aligned}$$

$$\gamma_I = \tan^{-1}\frac{B_I}{A_I},\quad \delta_I = \tan^{-1}\frac{D_I}{C_I},$$

and in mode II, Fig. 5, is as follows,

$$v_{II}(t) = \frac{\sqrt{2}\,V}{2\pi}\left\{\sqrt{A_{II}^2+B_{II}^2}\sin(\omega t+\gamma_{II})+\sum\frac{1}{k^2-1}\sqrt{C_{II}^2+D_{II}^2}\sin(k\omega t+\delta_{II})\right\} \tag{3}$$

where

$$A_{II} = 3\left\{\beta'\cos\alpha-\sin\beta'\cos\left(\alpha+\beta'+\frac{\pi}{3}\right)\right\}$$

$$B_{II} = 3\left\{\beta'\sin\alpha+\sin\beta'\sin\left(\alpha+\beta'+\frac{\pi}{3}\right)\right\}$$

$$C_{\text{II}} = \sqrt{3}\Big[\sin(\alpha+\beta')\Big\{-2\sin\left(k\beta'+\frac{\pi}{6}k\right)\cos\frac{\pi}{6}k-2\sqrt{3}\,k\cos\left(k\beta'+\frac{\pi}{6}k\right)\cos\frac{\pi}{6}k\Big\}$$

$$+\cos(\alpha+\beta')\Big\{2\sqrt{3}\sin\left(k\beta'+\frac{\pi}{6}k\right)\cos\frac{\pi}{6}k-2k\cos\left(k\beta'+\frac{\pi}{6}k\right)\cos\frac{\pi}{6}k\Big\}$$

$$+\sin\alpha\left(\sin\frac{\pi}{3}k+\sqrt{3}\,k+\sqrt{3}\,k\cos\frac{\pi}{3}k\right)$$

$$+\cos\alpha\left(\sqrt{3}\sin\frac{\pi}{3}k+k+k\cos\frac{\pi}{3}k\right)\Big]$$

$$D_{\text{II}} = \sqrt{3}\Big[\sin(\alpha+\beta')\Big\{-2\cos\left(k\beta'+\frac{\pi}{6}k\right)\cos\frac{\pi}{6}k-2\sqrt{3}\,k\sin\left(k\beta'+\frac{\pi}{6}k\right)\cos\frac{\pi}{6}k\Big\}$$

$$+\cos(\alpha+\beta')\Big\{2\sqrt{3}\cos\left(k\beta'+\frac{\pi}{6}k\right)\cos\frac{\pi}{6}k-2k\sin\left(k\beta'+\frac{\pi}{6}k\right)\cos\frac{\pi}{6}k\Big\}$$

$$+\sin\alpha\left(1+\cos\frac{\pi}{3}k-\sqrt{3}\,k\sin\frac{\pi}{3}k\right)$$

$$+\cos\alpha\left(-\sqrt{3}-\sqrt{3}\cos\frac{\pi}{3}k-k\sin\frac{\pi}{3}k\right)\Big]$$

$$\gamma_{\text{II}} = \tan^{-1}\frac{B_{\text{II}}}{A_{\text{II}}}, \qquad \delta_{\text{II}} = \tan^{-1}\frac{D_{\text{II}}}{C_{\text{II}}}$$

conducting angle β' for line-to-line voltage rerfers to dotted line in Fig. 3,

and $\qquad k = 6n+1\,,\quad 6n+3\,,\quad 6n+5\,,\qquad (n=0, 1, 2, 3, \cdots)\,.$

The voltage waveshape contains only odd harmonics in a three-phase system. And the $(6n+1)$th harmonics are of positive sequence nature, the $(6n+5)$th harmonics have negative sequence nature while the $(6n+3)$th harmonics have a zero sequence nature. Calculated results of eq. (2) and eq. (3) are shown in Fig. 8.

On this calculation, in the area of FGHF in Fig. 3, β' is always equal to $\frac{\pi}{3}$, and in this case $\sqrt{C_{\text{II}}^2+D_{\text{II}}^2}$, eq. (3), is independent of α, i.e. the harmonic components become constant with α variation.

3-3. **Harmonic Circuit and Analysis of Characteristics**

The equivalent circuit per phase for kth harmonic is shown in Fig. 9.

The differences between this circuit compared to the circuit at fundamental line frequency are those needed to take account the harmonic frequency, i.e. for a time harmonic of order k, as follows,

(a) all reactances are evaluated at the harmonic frequency kf_1, where f_1 is the fundamental frequency.

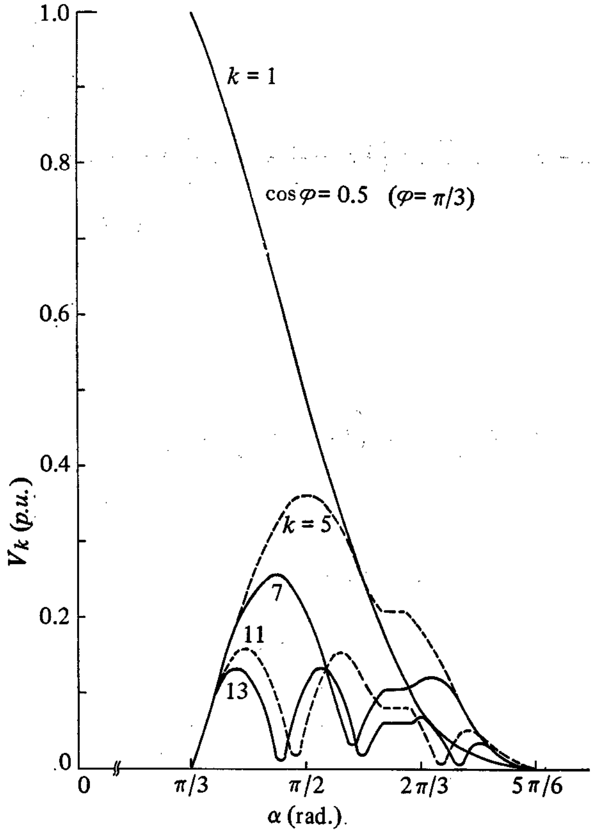

Fig. 8. Harmonic voltage components for inductive load.

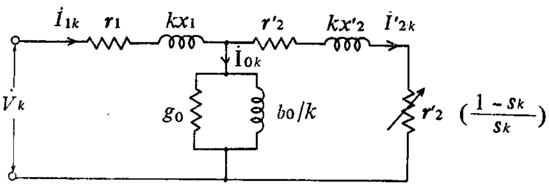

Fig. 9. Equivalent circuit for kth time harmonic.

(b) the slip is the harmonic slip s_k, and s_k is given as follows,

if synchronous speed of fundamental field $= N_s$

synchronous speed of kth harmonic $= kN_s$

rotor speed $= N$

fundamental slip, $s = \dfrac{N_s - N}{N_s}$

$$k\text{th harmonic slip, } s_k = \frac{kN_s \pm N}{kN_s} = \frac{k \pm (1-s)}{k} \qquad (4)$$

where positive sign is for the $(6n+5)$th harmonics and negative sign is for the $(6n+1)$ th harmonics,

kth harmonic secondary frequency, $f_{2k}=s_k k f_1$

$$=\{k\pm(1-s)\}f_1 \quad (5)$$

when s is small or $k\gg(1-s)$, $s_k\simeq 1$ and $f_{2k}\simeq kf_1$ (6)

In order to apply analytical methods based on the principle of superposition, certain simplifying assumptions are made regarding the motor.

(1) The rotor has not the structure of double squirrel-cage or deep-slot squirrel-cage.

(2) V_k does not become over the rated voltage.

(3) Saturation, hysteresis and eddy currents are ignored.

Considering $\dot{Z}_{1k}$, $\dot{Z}_{2k}$, and $\dot{Y}_k$ as follows,

$$\dot{Z}_{1k}=r_1+jkx_1\,,\quad \dot{Z}_{2k}=r_2'+js_k kx_2\,,\quad \dot{Y}_k=g_0-j\frac{b_0}{k} \quad (7)$$

each characteristic is given in eqs. (8)～(13).

exiciting current, $$\dot{I}_{0k}=\dot{V}_k\frac{s_k}{\dot{Z}_{2k}+s_k\dot{Z}_{1k}+\dot{Z}_{1k}\dot{Z}_{2k}\dot{Y}_k} \quad (8)$$

primary current, $$\dot{I}_{1k}=\dot{V}_k\frac{s_k+\dot{Z}_{2k}\dot{Y}_k}{\dot{Z}_{2k}+s_k\dot{Z}_{1k}+\dot{Z}_{1k}\dot{Z}_{2k}\dot{Y}_k}\equiv(A_k-jB_k)\dot{V}_k \quad (9)$$

secondary current, $$\dot{I}'_{2k}=\dot{V}_k\frac{\dot{Z}_{2k}\dot{Y}_k}{\dot{Z}_{2k}+s_k\dot{Z}_{1k}+\dot{Z}_{1k}\dot{Z}_{2k}\dot{Y}_k} \quad (10)$$

porwer factor, $$\cos\varphi_k=\frac{A_k}{\sqrt{A_k^2+B_k^2}} \quad (11)$$

primary input power, $$P_{ik}=3|\dot{V}_k|\,|\dot{I}_k|\cos\varphi_k \quad (12)$$

output power, $$P_k=3(I'_{2k})^2\frac{r_2'}{s_k}(1-s_k) \quad (13)$$

This is only the analysis for kth harmonic. So, if the supply voltage contains various harmonics, the primary current is obtained by taking the square root of the sum of the squares of all harminic currents.

primary current, $$|\dot{I}_1|=\sqrt{\sum_k|\dot{I}_{1k}|^2} \quad (14)$$

Similary:

primary voltage, $$|\dot{V}_1|=\sqrt{\sum_k|\dot{V}_k|^2} \quad (15)$$

primary input power, $$P_i=\sum_k P_{ik} \quad (16)$$

output power, $$P=\sum_k P_k \quad (17)$$

efficiency. $$\eta = \frac{P}{P_i} \tag{18}$$

power factor, $$\cos\varphi = \frac{P_i}{\sqrt{3}\,|\dot{I}_1|\,|\dot{V}_1|} \tag{19}$$

Therefore by knowing the rate of the vlotage for aech harmonic from Fig. 8, each characteristic is obtained.

Calculated characteristics are shown in Fig. 10, where triggering angle $\alpha = \frac{\pi}{2}$, stator line-to-line voltge (rms), $V_L = 150$ (V), and equivalent circuit constants are as follows,

$$r_1 = 0.827\,(\Omega)\,,\quad r_2' = 0.784\,(\Omega)\,,\quad x_1 = x'_2 = 1.505\,(\Omega)$$
$$g_0 = 0.002\,(\mho)\,,\quad b_0 = 0.024\,(\mho)\,.$$

Characteristics for sinusoidal operation with the same line-to-line voltage are given in dotted line.

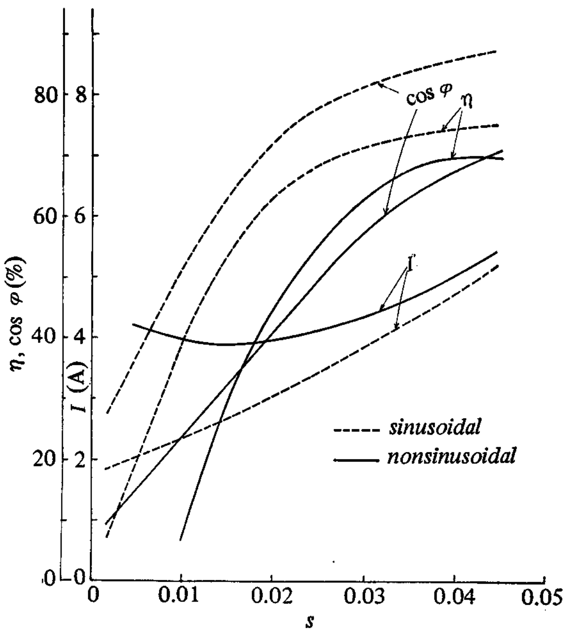

Fig. 10. Calculated characteristics of a three-phase induction motor.

4. Conclustion

The losses of an induction motor with nonsinusoidal waveforme impressed upon its terminals can be markedly different from its sinusoidal losses, depending upon the harmonic content of the impressed waveform.[11),12)] The most noticeable consequence of time harmonics is the increase in motor losses. The harmonic-produced steady-state torques are usually small and can be neglected in comparision with the fundamental torque. As the harmonic slip s_k, eq, (6), is nearly equal to unity for higher harmonics, the motor is locked rotor condition, the harmonic components can scarcely produce torques.

The motor can smoothly be controlled only for mode I. And near the boundary of the mode I and mode II, the motor performance becomes unstable. In mode II, the motor is forced to drive in single-phase operation. Therefore it is desirable to control in the region of mode I.

From eq. (6), the kth harmonic secondary frequency, $f_{2k} \simeq kf_1$, this means that the secondary frequency is very high. When the supply voltage is rich in harmonics, the circuit constants become nonlinear by the influence of skin effect.[13),14)] In particular, the secondary resistance, which disturbs the characteristics of the motor, cannot be held constant, but increases with frequency.

This effect will be presented in another paper.

References

1) Bradley, D.A., Clark, C.D., Davis, R.M., and Jones, D.A., PIEE **111**, 1833 (1964).
2) K.Y.G. Li, PIEE **116**, 1571 (1969).
3) P.L. Alger and Y.H. Ku, IEEE Trans., PAS-**76**, 1335 (1957).
4) G.C. Jain, IEEE Trans., PAS-**83**, 561 (1964).
5) Shepherd, W. and J. Stanly, IEEE Internat'l Conv. Rec., Pt **4**, 155 (1964).
6) Shepherd, W. and J. Stanly, ibid., 135 (1964).
7) Shepherd, W., IEEE Trans., IGA-**4**, 304 (1968).
8) Derek A., Paice, IEEE Trans., PAS-**87**, 585 (1968).
9) T. Fujii and T. Ishizaki, Lecture in Annual Meeting of Kansai Branch of I.E.E of Japan (1969).
10) M. Watanabe, T. Fujii, and T. Ishizaki, Lecture in Annual Meeting of I.E.E of Japan (1971).
11) Eugene A. Klingshirn, and Howard E. Jordan, IEEE Trans., PAS-**87**, 624 (1968).
12) B.J. Chalmers, and B.R. Sarkar, PIEE **115**, 1777 (1968).
13) M. Watanabe, T. Fujii, and T. Ishizaki, Lecture in Annual Meeting of Kansai Branch of I.E.E of Japan (1970).
14) T. Fujii, M. Watanabe, and T. Ishizaki, Lecture in Annual Meeting of I.E.E of Japan (1970).